doi:10.1016/S0022-2836(03)00275-4 J. Mol. Biol. (2003) 328, 409–418

JMB

Available online at www.sciencedirect.com

SCIENCE DIRECT®

Probing Catalytically Essential Domain Orientation in Histidine Kinase EnvZ by Targeted Disulfide Crosslinking

Sheng-Jian Cai[1], Ahmad Khorchid[2], Mitsuhiko Ikura[2] and Masayori Inouye[1]*

[1]*Department of Biochemistry Robert Wood Johnson Medical School, University of Medicine and Dentistry of New Jersey NJ 08854, USA*

[2]*Division of Molecular and Structural Biology Ontario Cancer Institute and Department of Medical Biophysics, University of Toronto, Toronto, Ont., Canada M5G 2M9*

**Corresponding author*

EnvZ, a dimeric transmembrane histidine kinase, belongs to the family of His-Asp phosphorelay signal transduction systems. The cytoplasmic kinase domain of EnvZ can be dissected into two independently functioning domains, A and B, whose NMR solution structures have been individually determined. Here, we examined the topological arrangement of these two domains in the EnvZ dimer, a structure that is key to understanding the mechanism underlying the autophosphorylation activity of the kinase. A series of cysteine substitution mutants were constructed to test the feasibility of chemical crosslinking between the two domains. These crosslinking data demonstrate that helix I of domain A of one subunit in the EnvZc dimer is in close proximity to domain B of the other subunit in the same dimer, while helix II of domain A of one subunit interacts with domain B of the same subunit in the EnvZc dimer. This is the first demonstration of the topological arrangement between the central dimerization domain containing the active center His residues (domain A) and the ATP-binding catalysis assisting domain (domain B) in a class I histidine kinase.

Keywords: histidine kinase; signal transduction; structure modeling; disulfide crosslinking; osmoregulation

Introduction

The EnvZ/OmpR His-Asp phosphorelay (HAP) signal transduction system regulates the expression of the major outer membrane porin genes, *ompC* and *ompF* in response to medium osmolarity changes in *Escherichia coli*.[1–3] EnvZ, a homodimeric transmembrane histidine kinase/phosphatase, *trans*-autophosphorylates the conserved His243 residue by using ATP.[4,5] Similar *trans*-phosphorylation of a histidine kinase is also observed in nitrogen regulator II (NRII).[6] The high-energy phosphoryl group is then transferred to the conserved Asp55 residue of its cognate response regulator OmpR.[7–9] The phosphorylated OmpR (OmpR-P) in turn binds to the upstream promoter regions of *ompC* and *ompF*genes, and reciprocally regulates the expression of the two genes.

EnvZ consists of four major domains, a receptor domain, a transmembrane domain, a linker region and a cytoplasmic kinase domain referred to as EnvZc (residues 180-450).[10] The EnvZc domain can be further dissected into two independent sub-domains, domain A and B.[11] Domain A (residues 223-289), also called the DHp (dimerization and histidine phosphotransfer) domain, contains the autophosphorylation site (His243 residue) and functions as the dimerization domain in EnvZ. Domain B (residues 290-450), also known as the CA (catalysis-assisting and ATP-binding) domain, binds ATP and contains conserved sequences such as F, N, G1, G2 and G3 boxes, which exist in all members of the histidine kinase family.[12–14] The NMR solution structures of domain A and domain B have been solved.[15,16] Domain A of EnvZ is a homodimer in which each subunit forms a hairpin motif with a turn region between two helixes and the two subunits associate to form a four-helix bundle (Figure 1(A)). Domain B of EnvZ is monomeric and shows a 4α/5β sandwich fold (Figure 1(B)). To date, no X-ray or NMR structure is available for EnvZc. Domain A, containing the His243

Abbreviations used: OmpR-P, phosphorylated OmpR; NRII, nitrogen regulator II.

E-mail address of the corresponding author: inouye@umdnj.edu

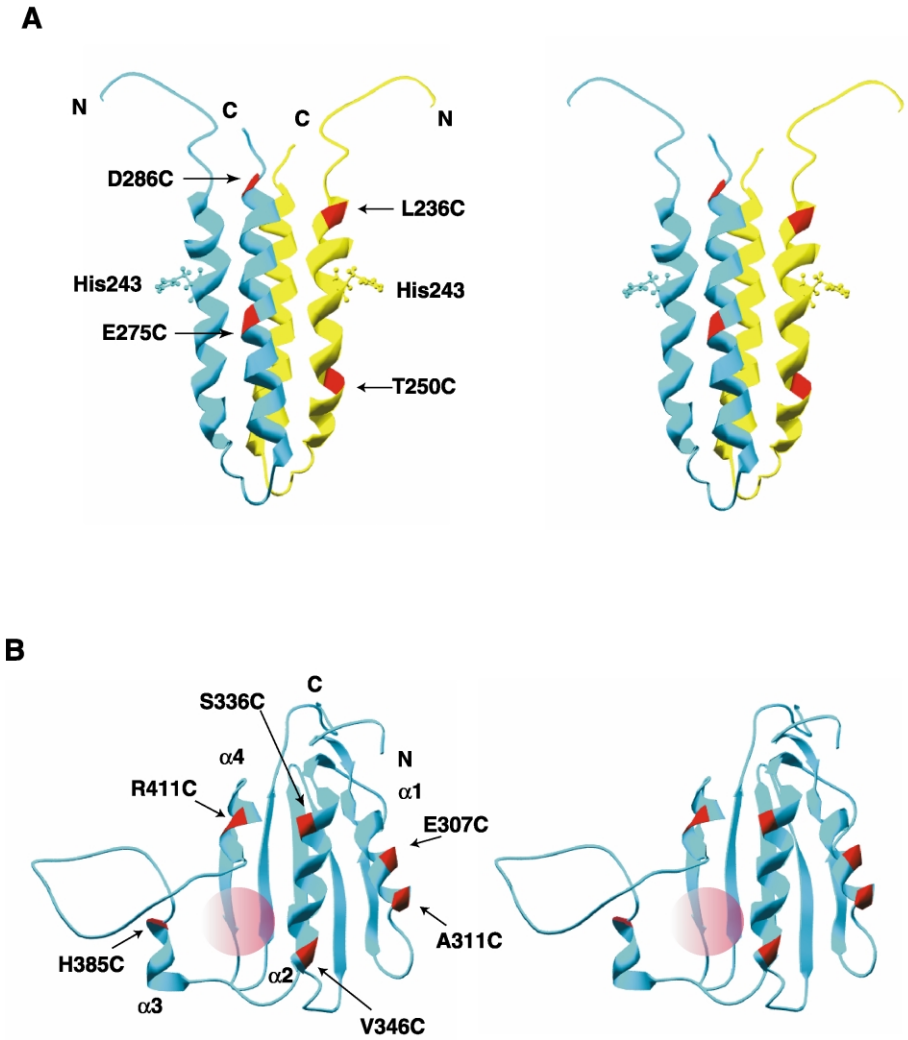

Figure 1. Positions of cysteine substitutions on domain A and domain B. A, Stereo-view of the solution structure of a domain A of EnvZ indicating positions of His243 and cysteine substitutions L236C, T250C, E275C and D286C as indicated. One subunit is shown in yellow while the other is in cyan. The N-terminal end of each subunit is also indicated. B, Stereo-view of the solution structure of domain B of EnvZ indicating cysteine substitutions E307C, A311C, S336C, V346C, H385C and R411C. The four α-helices of domain B are as indicated (α1, α2, α3, α4) and the N-terminal end is also shown. The ATP-binding site is represented by a pink sphere.

phosphorylation site, can be phosphorylated by adding domain B together with ATP, while domain A alone is sufficient to dephosphorylate OmpR-P in the presence of Mg^{2+}. Note that domain B does not have phosphatase activity, but can slightly stimulate domain A's phosphatase activity in the presence of ADP.[17] By comparing the phosphatase activity of domain A and EnvZc, it has been proposed that the phosphatase activity of EnvZ is regulated by the spatial arrangement between the covalently linked domain A and domain B, however the topological relationship between domain A and domain B remains to be elucidated.

Targeted disulfide crosslinking has been widely used for the study of protein structure and function. This approach has been used to define the domain structure, surface accessibility and spatial proximity of specific residues in Tar, a chemoreceptor for aspartate,[18] and to probe the ligand-induced conformational changes in the Tar receptor.[19] Targeted disulfide crosslinking has also been used to investigate the structure of the transmembrane regions of Tar[20] and various other proteins, including the ribose/galactose receptor Trg,[21,22] and lactose permease,[23] as well as to study dimerization of Hin recombinase.[24] One major advantage resulting from the application of this approach to study the spatial relationship between domain A and domain B of EnvZ, is that disulfide crosslinking not only shows which residues between domain A and domain B are in proximity but also reveals whether this spatial relationship between the two residues is within the same subunit in a dimer (intra-molecular) or between the two different subunits in a dimer (inter-molecular). Here, we introduced a series of

Table 1. Enzymatic activities of His_6-EnvZc cysteine substitution mutants

		Autokinase	Omp R-Kinase	Omp R-P Phosphatase
1	His_6-EnvZc (wt)	++++	++++	++++
2	His_6-EnvZc-1	++++	++++	+++
3	L236C	++++	++++	++
4	T250C	+++	+++	++
5	E275C	+++	+++	++
6	D286C	+++	++++	++
7	S336C	+++	++++	+++
8	V346C	+++	+++	+
9	H385C	+++	++++	++
10	R411C	+++	+++	++
11	L236C/S336C	+++	++++	++
12	L236C/R411C	+++	++++	++
13	T250C/H385C	+++	+++	++
14	T250C/V346C	+++	+++	+
15	E275C/V346C	+++	+++	+
16	E275C/A311C	+++	+++	++
17	D286C/S336C	+++	++++	++
18	D286C/E307C	+++	+++	+

Enzymatic activities of wild-type His_6-EnvZc are considered as 100%. +, ++, +++, ++++ represent approximately 25%, 50%, 75% and 100% of enzymatic activities compared to wild-type His_6-EnvZc

cysteine substitutions (see Figure 1) into each domain of the EnvZc dimer and performed crosslinking experiments by oxidizing of a pair of cysteine residues. Based on the subsequent disulfide bridge formation in a number of mutant homodimers, we propose a model for the topological relationship between domain A and domain B.

Results

Biochemical activities of His_6-EnvZc mutants

Since EnvZc has a cysteine residue at position 277, this residue was first substituted to Ser in His_6-EnvZc to eliminate multiple reaction sites in the chemical crosslinking. All cysteine substitution mutations were introduced into the His_6-EnvZc(C277S) (His_6-EnvZc-1) construct. The biochemical activities of His_6-EnvZc-1 mutant proteins containing the cysteine substitutions were first examined (Table 1). Note that the C277S mutation did not affect the enzymatic activities of His_6-EnvZc. All single and double cysteine substitutions examined retained significant levels of both autokinase and OmpR kinase activities while most of them have reduced levels of OmpR-P phosphatase activity. The V346C mutation, which is located in close proximity to the ATP binding site in domain B severely affected the phosphatase activity compared with other single cysteine substitution mutant proteins. It should be noted that OmpR-P phosphatase activity is known to be very sensitive to subtle conformational changes induced by mutations in EnvZc.[5] As no significant changes in autokinase and OmpR-kinase activities have been detected, most of the cysteine substitutions are therefore not likely to significantly affect the overall conformation of the His_6-EnvZc protein.

Crosslinking between helix II of domain A and domain B

To examine the interaction between helix II of domain A and helix α2 of domain B in the EnvZc dimer, the double cysteine substitutions E275C/V346C and D286C/S336C were introduced into His_6-EnvZc-1 (see Figure 1 for the positions of the helices and cysteine substitutions). The purified His_6-EnvZc-1(E275C/V346C) protein was dialyzed in 1000 X volume of buffer B for two hours at 4 °C and then subjected to SDS-PAGE with (lane 3, Figure 2(A)) or without (lane 2, Figure 2(A)) β-mercaptoethanol as described in Materials and Methods. The SDS-PAGE gels were then stained with Coomassie brilliant blue. As shown in lane 2, Figure 2(A), when oxidized a significant amount of His_6-EnvZc-1(E275C/V346C) migrated faster at position (a) than the non-oxidized protein at position (b) (lane 1, Figure 2(A)), indicating that intra-molecular crosslinking within a single molecule resulted in a faster mobility relative to the reduced molecule in the SDS-PAGE gel. When the oxidized His_6-EnvZc-1(E275C/V346C) protein was treated with β-mercaptoethanol, the mobility of the protein was restored to the original position (b) as shown in lane 3, Figure 2(A). This result indicates that Glu275 in helix II of domain A is in close proximity to Val346 on helix α2 of domain B of the same subunit in the EnvZ dimer.

The purified His_6-EnvZc-1(D286C/S336C) protein was treated in the same way as His_6-EnvZc-1(E275C/V346C). As indicated by the faster mobility (position (a)) of the oxidized protein in lane 5, Figure 2(A), a disulfide bond was formed within the same subunit of His_6-EnvZc-1(D286C/S336C). After treatment with β-mercaptoethanol, the crosslinked His_6-EnvZc-1(D286C/S336C) mobility reverted back to position (b) in lane 6, Figure 2(A), identical to the non-oxidized control

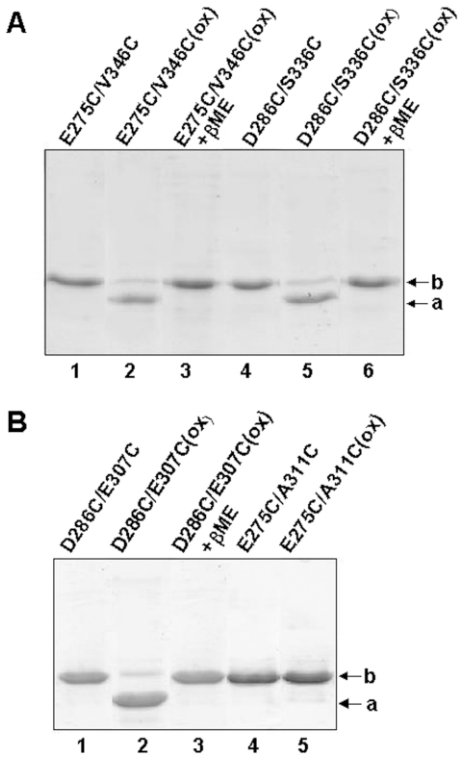

Figure 2. Disulfide crosslink formation between helix II of domain A and domain B. EnvZc mutant proteins containing cysteine substitutions were crosslinked as described in Materials and Methods and then subjected to SDS-PAGE. The SDS-PAGE gel was stained with Coomassie brilliant blue. A, Lane 1, non-oxidized His_6-EnvZc-1(E275C/V346C); lane 2, oxidized His_6-EnvZc-1(E275C/V346C); lane 3, oxidized His_6-EnvZc-1(E275C/V346C) treated with β-mercaptoethanol; lane 4 non-oxidized His_6-EnvZc-1(D286C/S336C); lane 5, oxidized His_6-EnvZc-1(D286C/S336C); and lane 6, oxidized His_6-EnvZc-1 (D286C/S336C) treated with β-mercaptoethanol. B, Lane 1, non-oxidized His_6-EnvZc-1(D286C/E307C); lane 2, oxidized His_6-EnvZc-1(D286C/E307C); lane 3, oxidized His_6-EnvZc-1(D286C/E307C) treated with β-mercaptoethanol; lane 4, non-oxidized His_6-EnvZc-1(E275C/A311C); lane 5, oxidized His_6-EnvZc-1(E275C/A311C). The positions of oxidized (a) and non-oxidized (b) forms of His_6-EnvZc-1 mutant proteins are indicated.

in lane 4. This result also suggests that Asp286 on helix II of domain A is in the proximity of Ser336 on helix α2 of domain B of the same subunit in the EnvZc dimer.

Then we examined the abilities of the two cysteine substitutions in helix II of domain A, E275C and D286C, to interact with helix α1 of domain B. Two double-cysteine substitution mutations, E275C/A311C and D286C/E307C were introduced into His_6-EnvZc-1. Crosslinking of His_6-EnvZc-1(E275C/A311C), and His_6-EnvZc-1 (D286C/E307C) was carried out as described in Materials and Methods. No crosslinking product of His_6-EnvZc-1(E275C/A311C) was detected (lane 5, Figure 2(B)). For His_6-EnvZc-1(D286C/E307C), only an intra-subunit crosslinked product at position (a) was formed (lane 2, Figure 2(B)), indicating that D286C in helix II of domain A is close to E307C in helix α1 of domain B within the same subunit. β-Mercaptoethanol treatment of the oxidized His_6-EnvZc-1(D286C/E307C) yielded a band at position (b) (lane 3, Figure 2(B)), the same position as the non-crosslinked control in lane 1.

Since D286C was able to crosslink with both S336C and E307C, Asp286 in helix II of domain A is considered to be in the proximity of Ser336 in helix α2 of domain B and Glu307 in helix α1 of domain B within the same subunit of EnvZc. Oxidation of His_6-EnvZc-1(E275C/A311C) resulted in no disulfide bond formation (lane 5, Figure 2(B)), as evident by comparison with the non-oxidized sample in lane 4, Figure 2(B), indicating that Glu275 is in close proximity to Val346 but not to Ala311 within the same subunit in the EnvZc dimer.

Crosslinking between helix I of domain A and domain B

We next examined the spatial relationship between helix I of domain A and domain B. Based on our crosslinking results between E275C and V346C, D286C and S336C, and D286 and E307, Leu236 on helix I of domain A is speculated to be close to Arg411 on helix α4 of domain B of the other subunit, and Thr250 on helix I of domain A close to the ATP-binding site in domain B of the other subunit in the EnvZ dimer (Figure 1). To further examine this, three double cysteine substitutions, L236C/R411C, T250C/V346C and T250C/H385C, were introduced into His_6-EnvZc-1.

Since there are two pairs of L236C and R411C in the His_6-EnvZc-1(L236C/R411C) dimer, it is possible to form either one or two disulfide bond(s) between the two subunits, which may result in two dimer bands on an SDS-PAGE gel. Indeed as shown in lane 8, Figure 3(A), two dimer bands (marked with 1 and 2) are observed, indicating the formation of inter-subunit disulfide crosslinking between L236C and R411C. When the oxidized His_6-EnvZc-1(L236C/R411C) protein was treated with β-mercaptoethanol, only a single band (lane 9, Figure 3(A)), which migrated at the same position as the non-oxidized control (lane 7, Figure 3(A)) was observed. The two dimer bands, 1 and 2, were dissected from the SDS-PAGE gel. One half of each band was treated in 50 mM β-mercaptoethanol for ten minutes at 37 °C and the other half was treated in 200 mM β-mercaptoethanol for ten minutes at 37 °C. Both were then subjected to SDS-PAGE. As shown in lanes 10 and 11, Figure 3(A), both 50 mM and 200 mM β-mercaptoethanol treatment almost completely converted band 1 to the monomer band. On the other hand, in 50 mM β-mercaptoethanol, the density of band 2 was significantly reduced, with concomitant appearance of band 1 as well as the monomer band as shown in lane 12, Figure 3(A). When treated with 200 mM β-mercaptoethanol, most of band 2 was

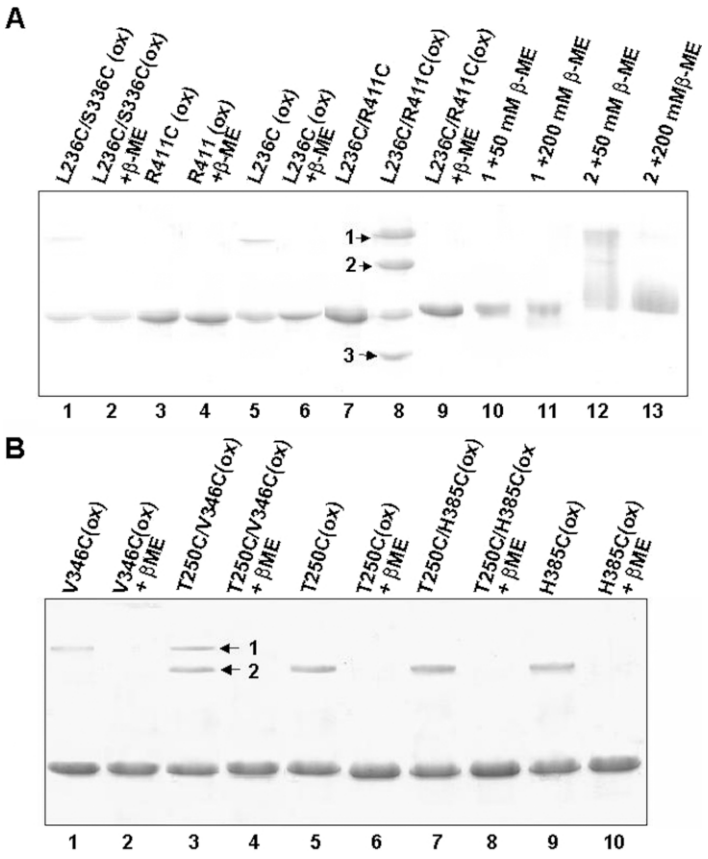

Figure 3. Disulfide crosslink formation between helix I of domain A and domain B. EnvZc mutant proteins containing cysteine substitutions were crosslinked as described in Materials and Methods and then subjected to SDS-PAGE. The SDS-PAGE gel was stained with Coomassie brilliant blue. A, Lane 1, oxidized His_6-EnvZc-1(L236C/S336C); lane 2, oxidized His_6-EnvZc-1(L236C/S336C) treated with β-mercaptoethanol; lane 3, oxidized His_6-EnvZc-1(R411C); lane 4, oxidized His_6-EnvZc-1(R411C) treated with β-mercaptoethanol; lane 5, oxidized His_6-EnvZc-1(L236C); lane 6, oxidized His_6-EnvZc-1(L236C) treated with β-mercaptoethanol; lane 7, non-oxidized His_6-EnvZc-1(L236C/R411C); lane 8, oxidized His_6-EnvZc-1(L236C/R411C); lane 9, oxidized His_6-EnvZc-1(L236C/R411C) treated with β-mercaptoethanol; lane 10, dimer band 1, as indicated in lane 8, treated with 50 mM β-mercaptoethanol for ten minutes at 37 °C; lane 11, dimer band 1 treated with 200 mM β-mercaptoethanol for ten minutes at 37 °C; lane 12, dimer band 2, as indicated in lane 8, treated with 50 mM β-mercaptoethanol for ten minutes at 37 °C; lane 13, dimer band 2 treated with 200 mM β-mercaptoethanol for ten minutes at 37 °C. B, Lane 1, oxidized His_6-EnvZc-1(V346C); lane 2, oxidized His_6-EnvZc-1(V346C) treated with β-mercaptoethanol; lane 3, oxidized His_6-EnvZc-1(T250C/V346C); lane 4, oxidized His_6-EnvZc-1(T250C/V346C) treated with β-mercaptoethanol; lane 5, oxidized His_6-EnvZc-1(T250C); lane 6, oxidized His_6-EnvZc-1(T250C) treated with β-mercaptoethanol; lane 7, oxidized His_6-EnvZc-1(T250C/H385C); lane 8, oxidized His_6-EnvZc-1(T250C/H385C) treated with β-mercaptoethanol; lane 9, oxidized His_6-EnvZc-1(H385C); lane 10, oxidized His_6-EnvZc-1(H385C) treated with β-mercaptoethanol.

converted to the monomer band (lane 13, Figure 3(A)). These results indicate that the band 2 dimer contains two disulfide bonds while the band 1 dimer has one.

Crosslinking between L236C and R411C also produced another band at position 3 as shown in lane 8, Figure 3(A). Since this band migrated faster than the monomer band, it is considered to have resulted from intra-subunit crosslinking. This may be due to the dynamic nature of EnvZc that allows Arg411 to be also close to Leu236 in the same subunit. However, as shown in Figure 4 later, the inter-subunit crosslinked His_6-EnvZc-1(L236C/R411C) protein retained the autokinase and OmpR-kinase activities while the intra-subunit crosslinked one did not, indicating that Leu236 in domain A is in close proximity to Arg411 in domain B of the other subunit in the functional EnvZc dimer. As a control, crosslinking of His_6-EnvZc-1(L236C), a single cysteine substitution mutant, resulted in a weak inter-subunit crosslinked dimer band (lane 5, Figure 3(A)). On the other hand, crosslinking of His_6-EnvZc-1(R411C), another single cysteine substitution control, showed no disulfide bond formation (compare lanes 3 and 4, Figure 3(A)). We also examined the possible interaction between L236 and S336 in EnvZ. As shown in lanes 1 and 2, Figure 3(A), oxidized His_6-EnvZc-1(L236C/S336C) protein showed a weak dimer band, which is similar to oxidized His_6-EnvZc-1(L236C) (lane 5, Figure 3(A)), indicating that L236C does not form a disulfide bond with S336C. Therefore, Leu236 on helix I of domain A is in close proximity to the Arg411 on helix α4 but not to the Ser336 on helix α2 of domain B of the other subunit.

Oxidation of His_6-EnvZc-1(T250C/V346C) resulted in two weak dimer bands (1 and 2 in lane 3, Figure 3(B)). Band 1 was at the similar position of the dimer band formed by oxidizing His_6-EnvZc-1(V346C) (lane 1, Figure 3(B)), while band 2 was at the same position of the dimer band resulting from the oxidization of His_6-EnvZc-1(T250C) (lane 5, Figure 3(B)). This indicates that there was no disulfide bond formed between T250C and V346C. Crosslinking of His_6-EnvZc-1(T250C/H385C) yielded a dimer band (lane 7, Figure 3(B)), which migrated at a similar position

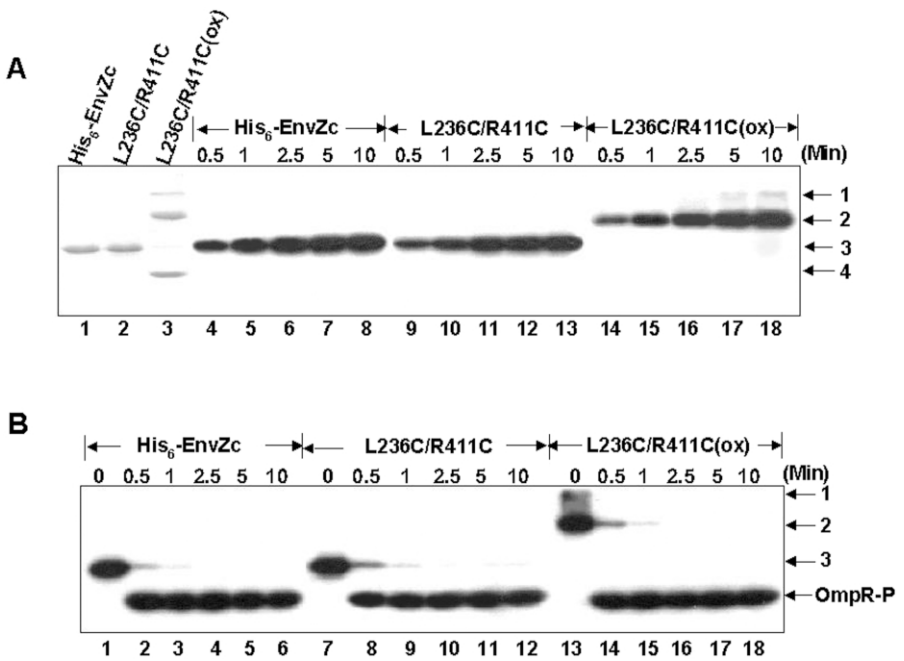

Figure 4. Autokinase and OmpR-kinase activities of crosslinked His_6-EnvZc-1 (L236C/R411C). Autokinase and OmpR-kinase assay were carried out as described [28]. His_6-EnvZc-1(L236C/R411C) protein was dialyzed in buffer B overnight. A, SDS-PAGE gel of 2 μg of His_6-EnvZc(wt) (lane 1), 2 μg of His_6-EnvZc-1(L236C/R411C) (lane 2), and 4 μg of oxidized His_6-EnvZc-1(L236C/R411C) (lane 3) stained with Coomassie brilliant blue. Lanes 4–18, an autoradiogram of a SDS-PAGE gel of the autokinase assays for His_6-EnvZc(wt) (lanes 4–8), His_6-EnvZc-1(L236C/R411C) (lanes 9–13), and oxidized His_6-EnvZc-1(L236C/R411C) (lanes 14–18). The proteins used in kinase assays and loaded on each lane were one fourth of the proteins loaded in lanes 1–3. The samples and the time periods after addition of [γ-^{32}P]ATP are as indicated on top of the gel. On the right side of the gel, the positions 1–4 are shown: band 1, single-inter-crosslinked His_6-EnvZc-1(L236C/R411C); band 2, double-inter-crosslinked His_6-EnvZc-1(L236C/R411C); band 3, non-crosslinked samples; band 4, intra-crosslinked His_6-EnvZc-1(L236C/R411C). B, An autoradiogram of a SDS-PAGE gel for OmpR-kinase assays. The protein samples and the time periods after addition of OmpR are indicated on top of the gel. Lanes 1–6, wild-type His_6-EnvZc; lanes 7–12, His_6-EnvZc-1(L236C/R411C); lanes 13–18, oxidized His_6-EnvZc-1(L236C/R411C). The positions 1–3 are shown at the right side of the gel: band 1, single-inter-crosslinked His_6-EnvZc-1(L236C/R411C); band 2, double-inter-crosslinked His_6-EnvZc-1 (L236C/R411C); band 3, non-crosslinked protein samples. The position of phosphorylated-OmpR (OmpR-P) band is also indicated.

compared to the dimer band of oxidized His_6-EnvZc-1(T250C) and the dimer band of oxidized His_6-EnvZc-1(H385C) (lane 9, Figure 3(B)). This suggests that T250C in domain A cannot be crosslinked with H385C in domain B. These results are consistent with the notion that Thr250 of domain A is close to the ATP-binding site but not to the Val346 or His385 of domain B. These data together with that from His_6-EnvZc-1(L236C/R411C) demonstrate that helix I of domain A of one subunit is in close proximity to domain B of the other subunit in the EnvZ dimer. The dimer bands observed in the single cysteine substitutions H385C, T250C and L236C, may be due to the disulfide bonds randomly formed between two dimers in the solution.

Autokinase and OmpR-kinase activity of crosslinked His_6-EnvZc-1(L236C/R411) mutant protein

The His_6-EnvZc-1(L236C/R411C) mutant protein was dialyzed overnight in order to obtain a higher yield of crosslinking. As shown in lane 3, Figure 4(A), two major bands were observed: band 2 for double-inter-crosslinked dimers and band 4 for intra-crosslinked monomers. This crosslinked preparation was then examined for autokinase activity (lanes 4-18, Figure 4(A)). Interestingly, the double-inter-crosslinked His_6-EnvZc-1(L236C/R411) (lanes 14–18, Figure 4(A)) showed a very similar autokinase activity to that of non-crosslinked protein (lanes 9–13, Figure 4(A)). The autokinase activities of both the oxidized and reduced forms were slightly weaker than that of the wild-type His_6-EnvZc (lanes 4–8, Figure 4(A)). When their phosphotransfer (OmpR kinase) activities were examined, however, it was found that there were no significant differences between wild-type His_6-EnvZc (lanes 1–6, Figure 4(B)), His_6-EnvZc-1(L236C/R411) (lanes 7–12, Figure 4(B)), and double-inter-crosslinked His_6-EnvZc-1(L236C/R411C) (lanes 13–18, Figure 4(B)). These results indicate that crosslinking between these two residues does not affect EnvZc enzymatic functions and further support the notion that Leu236 in helix I of domain A is in close proximity to Arg411 of domain B of the other subunit in the

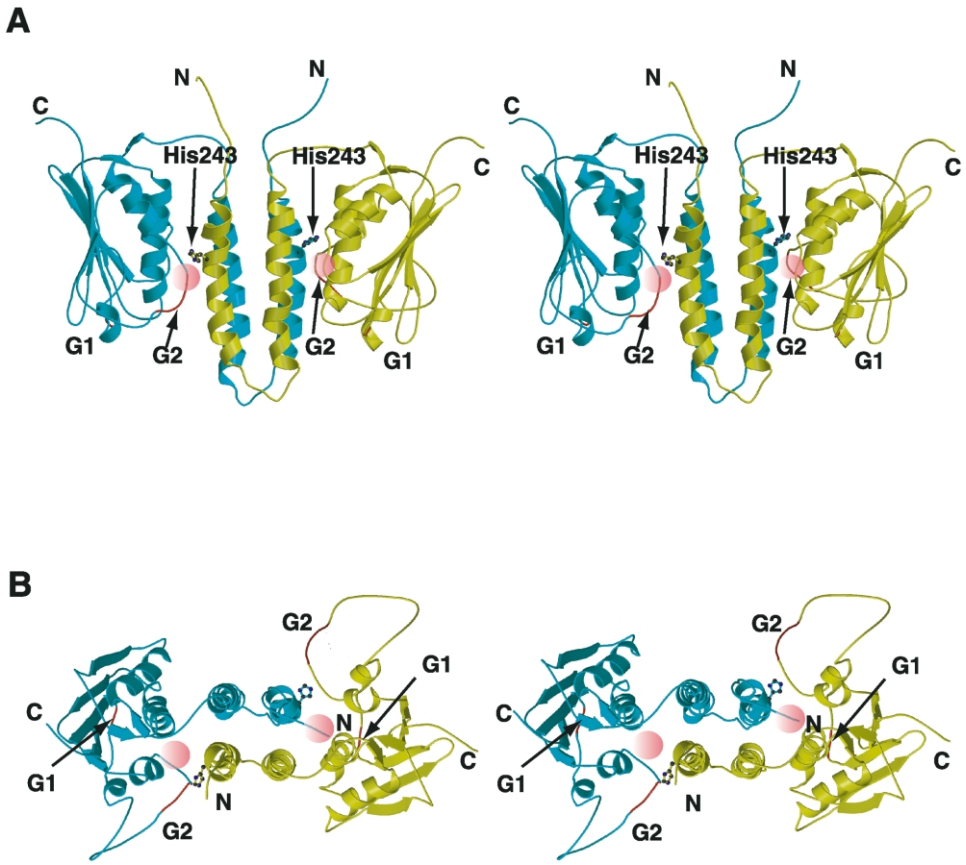

Figure 5. Proposed model of the EnvZc dimer. Front (A) and top (B) stereo-views of an EnvZc dimer. The two subunits are shown in yellow and cyan. The active site histidine side-chain (His243) is indicated while the ATP-binding site is represented by a pink sphere. The conserved G1 and G2 boxes are shown in red.

EnvZ dimer. It should be noted that the intra-crosslinked band (band 4) did not show any autokinase activity.

Structure modeling

In order to assess the validity of the chemical crosslinking data described above and to use these data to construct a plausible model that would satisfy all the chemical constraints, we performed computational modeling on EnvZc. First, we generated an initial structural model for EnvZc by joining two separate NMR-derived structures of domains A (1JOY) and B (1BXD). This initial model did not contain any restraints between the two domains, which could be freely rotated relative to one another. We then introduced chemical constraints between the following four pairs of amino acid residues: Leu236-Arg411, Glu275-Val346, Asp286-Ser336, and Asp286-Glu307. In light of a regular geometry of the disulfide bond found in protein structures,[25] a 10 Å restriction was used between the α carbons for each pair. Based on the *trans*-autophosphorylation mechanism for EnvZ kinase activity, an additional restraint between His243 on one monomer and the *trans* Asn347 on the other monomer was introduced. A total of 20 structures were calculated and a representative structure is shown in Figure 5. The average pair-wise root mean square (r.m.s.) deviation of the MODELLER-derived structures is 2.2 Å for the backbone atoms and 2.4 Å for all heavy atoms, excluding the N-terminal region from residue 223–232 and the C-terminal region from residue 443–450, which were unstructured in the NMR solution structures of domain A and domain B.

Discussion

Our crosslinking data yielded a structural model of EnvZc, that revealed the topological relationship between domain A and domain B of EnvZ. In this model, the ATP-binding face of domain B of one subunit packs against two helices of domain A, one provided by the same subunit and the other by the second subunit (Figure 5). This model of dimeric EnvZc supports the notion that dimer formation is essential for the function of EnvZ. It is important to note that His243 is located at the edge formed by the intra-subunit and inter-subunit surfaces and points to the ATP-binding site of domain B in this model. Another observation in the model is that domain B predominantly occupies the top half of the inter-subunit surface

but barely interacts with the intra-subunit surface. In this arrangement, EnvZc forms a six-helix bundle made up of a pair of helices I and II of dimeric domain A as well as helix α2 of domain B, which aligns anti-parallel to helix II of the same subunit (Figure 5). More quantitatively, the angle between helix α2 of domain B and helix II of domain A is 16.8 degrees and the distance between the two helices is 16.5 Å, demonstrating a close anti-parallel packing of the helices. The model also predicts a close proximity between the G2 box (residues 401–405) in domain B and the conserved His243 in domain A. Together with the G1 box (residues 375–377), the G2 box has been thought to be involved in ATP binding and catalysis. In the NMR-derived structure of domain B, the G2 box lies in the flexible loop region (residues 386–408) between helices α3 and α4, and therefore the exact location of the G2 box was ill defined.[15] The significance of this long flexible loop has long been in question, as different mutations in this region resulted in the reduction of either the kinase or phosphatase activity of EnvZ.[26] The present modeling study suggests that the flexible loop in domain B may be folded into a more rigid structure such that this region of one subunit can pack against the intra-subunit surface of domain A in the other subunit (Figure 5).

Comparison of this EnvZc model with the solved structures of the class II histidine kinase CheA shows several differences in the interaction between the dimerization and ATP-binding domains and in their relative positioning within the dimer. In CheA, the ATP-binding domain is positioned such that it interacts with the intra-subunit molecular surface of the dimer, whereas in the class I histidine kinase EnvZc, the ATP-binding domain B interacts with the inter-subunit surface. The observed differences in the relative positioning of the dimerization and kinase domains might be related to the fact that the conserved hinge region in the class I kinase EnvZ is longer than that in class II histidine kinases such as CheA. These differences in relative positioning of the domains and conserved hinge regions represent distinct structural characteristics of two different classes of histidine kinases, and indicate that the relative arrangement of the dimerization and kinase domains is an essential feature of the signaling mechanism.

The current model gives further insight into the possible functional mechanism of EnvZ. The inter-subunit surface of domain A predominantly serves as the binding site of domain B, and thus the intra-subunit surface of domain A may be used as the binding site for OmpR and OmpR-P. With this spatial domain arrangement, both the ATP-binding domain (domain B) of EnvZ and Asp57 of the regulatory domain of OmpR, might be able to form the active complex together with His243, the autophosphorylation site in domain A of EnvZ, to effectively facilitate both the autophosphorylation reaction in EnvZ and the phosphotransfer reaction from EnvZ to OmpR. A similar arrangement between EnvZ and OmpR-P is likely to be made for the phosphatase reaction to dephosphorylate OmpR-P. The lack of success in crystallization of EnvZc and the broad NMR spectra observed for EnvZc in solution suggest a dynamic nature for the interaction between domains A and B. It is therefore possible that the OmpR binding site on domain A may overlap with the interacting surface of domain A with domain B, and these dual protein-protein interactions centered at the active site His243 may occur alternately and transiently in the cell.

Materials and Methods

Constructions of plasmids expressing His_6-EnvZc proteins containing cysteine substitutions

The unique cysteine residue in EnvZ, Cys277, was eliminated *via* a serine substitution by site-directed mutagenesis using plasmid pPH001 coding for the wild-type His_6-EnvZc[27] as a template, primers 5′-AAAGATATCGAAGATCCAACGCCAT-CATTGAG-3′ and 5′-CTCAATGATGGCGTTGACTCTCGATATCTTT-3′ and *Pfu* polymerase (Stratagene). The resulting plasmid pHEc(C277S) encoding His_6-EnvZc(C277S) was used as a template for introduction of various cysteine substitutions by site-directed mutagenesis. The following single or double cysteine substitutions were introduced into His_6-EnvZc(277S) (as His_6-EnvZc-1, thereafter): L236C, T250C, E275C, D286C, S336C, V346C, H385C, R411C, L236C/R411C, L236/S336, T250/V346, T250C/H385C, E275C/V346C, E275C/A311C, D286C/S336C, and D286C/E307C. The pairwise primers for each cysteine substitution are as follows: 5′-GCGGATGACCGCACGTGTCTGATGCGGGGGTA-3′, 5′-TACCCCCGCCATCAGACACGTGCGGTCATCCGC-3′ for L236C; 5′-TTGCGCACGCCGCTGTGCCGTATTCGCCTGGCG-3′, 5′-CGCCAGGCGAATACGGCACAGCGGCGTGCGCAA-3′ for T250C; 5′-ATCAATAAAGATATCTGTGAGTCCAACGCCATC-3′, 5′-GATGGCGTGATCACAGATATCTTTATTGAT-3′ for E275C; 5′-ATTGAGCAGTTTATCGCTACCTGCGCACCGGG-3′, 5′-CCCGGTGCGCAGGTAGCAGATAAATGCTCAAT-3′ for D286C; 5′-AATGCAGTACTCGGTTGTGTGATTGTGCCGAA-3′, 5′-TTCGGCAGCAATCACACAACCGAGTACTGCATT-3′ for E307C; 5′-GGTGAGGTGATTGCTTGCGAAAGTGGCTATGAG-3′, 5′-CTCATAGCCACTTTCGCAAGCAATCACCTCACC-3′ for A311C; 5′-AAAATGCACCCGCTGTGCATCAAACGCGCGGTG-3′, 5′-CACCGCGCGTTGATGCACAGCGGGTGCATTTT-3′ for S336C; 5′-GTGGCGAATATGGTGTGCAACGCCGCCCGTTAT-3′, 5′-ATAACGGGCGGCGTTGCACACCATATTCGCCAC-3′ for V346C; 5′-CCGGAACAACGTAAGTGCCTGTTCCAGCCGTTT-3′, 5′-AAACGGCTGGAACAGGCACTTACGTTGTTCCGG-3′ for H385C; 5′-CTGGCAATTGTGCAGTGTATCGTGGATAACCAT-3′, 5′-ATGGTTATCCACGATACACTGCACAATTGCCAG-3′ for R411C; respectively.

Purification of His_6-EnvZc and His_6-EnvZc mutant proteins

Purification of His_6-EnvZc and His_6-EnvZc mutant proteins was carried out in the presence of 5 mM dithiothreitol (DTT) as described.[27] *E. coli* strain

BL21(DE3) was used for expression of the His_6-EnvZc proteins.

Biochemical activities of His_6-EnvZc proteins

The autophosphorylation of wild-type and mutant His_6-EnvZc, phosphorylation of OmpR and dephosphorylation of phosphorylated OmpR (OmpR-P) by these proteins were carried out as described.[28] For the oxidized His_6-EnvZc-1(L236C/R411) protein sample, no reducing agent was used in the reaction buffers and loading buffer.

Disulfide crosslinking

Protein samples were oxidized with ambient oxygen through dialysis. Aliquots of 10 μM of His_6-EnvZc-1 proteins containing various cysteine substitution mutations were dialyzed in 1000 × volume of buffer B (50 mM Tris–HCl (pH 8.0), 150 mM KCl, 5% (v/v) glycerol) for one hour at 4 °C. The buffer was changed once and dialysis was continued for another one hour. Oxidized (15 μl) samples were mixed with 3 μl of 6 × SDS loading buffer with or without 1.2 M β-mercaptoethanol, incubated in a boiling water bath for three minutes and subjected to SDS-PAGE.

Computational modeling

Modeling of the EnvZc structure was performed using the program MODELLER 4[29] implemented on a Silicon Graphics workstation. The NMR-derived solution structures of the homodimerization domain A (1JOY; residues 223–289) and catalytic domain B (1BXD; residues 290–450) of EnvZ were used as templates for the model building of the entire catalytic core (residues 223–450). No energy minimization was employed. Interhelical angles and distances were calculated using the program VGM (Vector Geometry Mapping).[30]

Protein Data Bank coordinates

The atomic coordinates have been deposited in the Protein Data Bank (PDB). The PDB ID code for EnvZc is 1NJV.

Acknowledgements

This work was supported by Grant GM 19043 from the National Institutes of Health (to Ma.I.) and a Canadian Institutes of Health Research grant (to Mi.I.). A.K. was supported by an AMGEN/OCI fellowship.

References

1. Pratt, L. & Silhavy, T. J. (1995). Porin regulation of *Escherichia coli*. In *Two-component Signal Transduction* (Hoch, J. & Silhavy, T. J., eds), pp. 105–107, American Society for Microbiology Press, Washington.
2. Forst, S. A. & Roberts, D. L. (1994). Signal transduction by the EnvZ-OmpR phosphotransfer system in bacteria. *Res. Microbiol.* **145**, 363–373.
3. Egger, L. A., Park, H. & Inouye, M. (1997). Signal transduction *via* the histidyl-aspartyl phosphorelay. *Genes Cells.* **2**, 167–184.
4. Yang, Y. & Inouye, M. (1991). Intermolecular complementation between two defective mutant signal-transducing receptors of *Escherichia coli*. *Proc. Natl Acad. Sci. USA*, **88**, 11057–11061.
5. Qin, L., Dutta, R., Kurokawa, H., Ikura, M. & Inouye, M. (2000). A monomeric histidine kinase derived from EnvZ, an *Escherichia coli* osmosensor. *Mol. Microbiol.* **36**, 24–32.
6. Ninfa, E. G., Atkinson, M. R., Kamberov, E. S. & Ninfa, A. J. (1993). Mechanism of autophosphorylation of *Escherichia coli* nitrogen regulator II (NRII or NtrB): trans-phosphorylation between subunits. PG-7024-32. *J. Bacteriol.* **7024-32**, 175.
7. Aiba, H., Mizuno, T. & Mizushima, S. (1989). Transfer of phosphoryl group between two regulatory proteins involved in osmoregulatory expression of the ompF and ompC genes in *Escherichia coli*. *J. Biol. Chem.* **264**, 8563–8567.
8. Igo, M. M. & Silhavy, T. J. (1988). EnvZ, a transmembrane environmental sensor of *Escherichia coli* K-12, is phosphorylated *in vitro*. *J. Bacteriol.* **170**, 5971–5973.
9. Forst, S., Delgado, J. & Inouye, M. (1989). Phosphorylation of OmpR by the osmosensor EnvZ modulates expression of the *ompF* and *ompC* genes in *Escherichia coli*. *Proc. Natl Acad. Sci. USA*, **86**, 6052–6056.
10. Park, H. & Inouye, M. (1997). Mutational analysis of the linker region of EnvZ, an osmosensor in *Escherichia coli*. *J. Bacteriol.* **179**, 4382–4390.
11. Park, H., Saha, S. K. & Inouye, M. (1998). Two-domain reconstitution of a functional protein histidine kinase. *Proc. Natl Acad. Sci. USA*, **95**, 6728–6732.
12. Dutta, R. & Inouye, M. (2000). GHKL, an emergent ATPase/kinase superfamily. *Trends Biochem. Sci.* **25**, 24–28.
13. Parkinson, J. S. & Kofoid, E. C. (1992). Communication modules in bacterial signaling proteins. *Annu. Rev. Genet.* **26**, 71–112.
14. Swanson, R. V., Alex, L. A. & Simon, M. I. (1994). Histidine and aspartate phosphorylation: two-component systems and the limits of homology. *Trends Biochem. Sci.* **19**, 485–490.
15. Tanaka, T., Saha, S. K., Tomomori, C., Ishima, R., Liu, D., Tong, K. I. *et al.* (1998). NMR structure of the histidine kinase domain of the *E. coli* osmosensor EnvZ. *Nature*, **396**, 88–92.
16. Tomomori, C., Tanaka, T., Dutta, R., Park, H., Saha, S. K., Zhu, Y. *et al.* (1999). Solution structure of the homodimeric core domain of *Escherichia coli* histidine kinase EnvZ. *Nature Struct. Biol.* **6**, 729–734.
17. Zhu, Y., Qin, L., Yoshida, T. & Inouye, M. (2000). Phosphatase activity of histidine kinase EnvZ without kinase catalytic domain. *Proc. Natl Acad. Sci. USA*, **97**, 7808–7813.
18. Falke, J. J. & Koshland, D. E., Jr (1987). Global flexibility in a sensory receptor: a site-directed cross-linking approach. *Science*, **237**, 1596–1600.
19. Chervitz, S. A., Lin, C. M. & Falke, J. J. (1995). Transmembrane signaling by the aspartate receptor: engineered disulfides reveal static regions of the subunit interface. *Biochemistry*, **34**, 9722–9733.
20. Pakula, A. A. & Simon, M. I. (1992). Determination of transmembrane protein structure by disulfide cross-linking: the *Escherichia coli* Tar receptor. *Proc. Natl Acad. Sci. USA*, **89**, 4144–4148.

21. Lee, G. F., Lebert, M. R., Lilly, A. A. & Hazelbauer, G. L. (1995). Transmembrane signaling characterized in bacterial chemoreceptors by using sulfhydryl cross-linking *in vivo*. *Proc. Natl Acad. Sci. USA*, **92**, 3391–3395.
22. Lee, G. F., Dutton, D. P. & Hazelbauer, G. L. (1995). Identification of functionally important helical faces in transmembrane segments by scanning mutagenesis. *Proc. Natl Acad. Sci. USA*, **92**, 5416–5420.
23. Sahin-Toth, M. & Kaback, H. R. (1993). Cysteine scanning mutagenesis of putative transmembrane helices IX and X in the lactose permease of *Escherichia coli*. *Protein Sci.* **2**, 1024–1033.
24. Lim, H. M. (1994). Analysis of subunit interaction by introducing disulfide bonds at the dimerization domain of Hin recombinase. *J. Biol. Chem.* **269**, 31134–31142.
25. Cai, X., Lin, J., Yang, G., Shi, F., Shen, W., Cai, Y. & Wu, X. (1999). Cloning of *Schistosoma japonicum* Chinese strain 22.6 kD membrane-associated protein (Sj-22.6) gene and its overproduction on *Escherichia coli*. *Chin. J. Biotechnol.* **15**, 7–13.
26. Hsing, W., Russo, F. D., Bernd, K. K. & Silhavy, T. J. (1998). Mutations that alter the kinase and phosphatase activities of the two-component sensor EnvZ. *J. Bacteriol.* **180**, 4538–4546.
27. Hidaka, Y., Park, H. & Inouye, M. (1997). Demonstration of dimer formation of the cytoplasmic domain of a transmembrane osmosensor protein, EnvZ, of *Escherichia coli* using Ni-histidine tag affinity chromatography. *FEBS Letters*, **400**, 238–242.
28. Dutta, R., Yoshida, T. & Inouye, M. (2000). The critical role of the conserved Thr247 residue in the functioning of the osmosensor EnvZ, a histidine Kinase/Phosphatase, in *Escherichia coli*. *J. Biol. Chem.* **275**, 38645–38653.
29. Sali, A. (1995). Comparative protein modeling by satisfaction of spatial restraints. *Mol. Med. Today*, **1**, 270–277.
30. Yap, K. L., Ames, J. B., Swindells, M. B. & Ikura, M. (2002). Vector geometry mapping. A method to characterize the conformation of helix-loop-helix calcium-binding proteins. *Methods Mol. Biol.* **173**, 317–324.

Edited by P. Wright

(Received 21 August 2002; received in revised form 15 January 2003; accepted 21 February 2003)